Local Structure and Polar Order in

Liquid N-methyl-2-pyrrolidone (NMP)

*N. S. Basma[1,2], T. F. Headen[3], Milo S. P. Shaffer[1], N.T. Skipper[2] and C. A. Howard[*2]*

[1]Department of Chemistry, Imperial College London, South Kensington, London SW7 2AZ, United Kingdom

[2]Department of Physics and Astronomy, University College London, London WC1E 6BT, United Kingdom

[3]ISIS Neutron and Muon Source, Rutherford Appleton Laboratory, Harwell Campus, Didcot, Oxfordshire OX11 0QX, United Kingdom

*To whom correspondence should be addressed. E-mail: c.howard@ucl.ac.uk

SI I: Neutron Diffraction Theory

Neutron diffraction is a well-established experimental technique through which the average local structure of hydrogen-containing compounds can be determined. Neutron scattering experiments measure the differential scattering cross-section. Following corrections, the total structure factor, $F(Q)$, which provides a direct measurement of the structure in reciprocal space, can be extracted. Q is the magnitude of the momentum change vector of the scattered neutrons and is given by:

$$Q = \frac{4\pi}{\lambda} \sin\theta \qquad , \qquad \text{(Eq. 1)}$$

where λ is the wavelength of neutrons incident onto the sample and 2θ is the scattering angle. F(Q) can be written as a sum of the Faber-Ziman partial structure factors, $S_{\alpha\beta}(Q)$:

$$F(Q) = \sum_{\alpha \leq \beta} (2 - \delta_{\alpha\beta}) c_\alpha c_\beta b_\alpha b_\beta (S_{\alpha\beta}(Q) - 1) \qquad , \qquad \text{(Eq. 2)}$$

weighted by the respective concentrations, c_α and c_β, and scattering lengths, b_α and b_β, of each atom type. The Kronecker delta function, $\delta_{\alpha\beta}$, is used to avoid double counting. The $S_{\alpha\beta}(Q)$ terms contain information about correlations between the atomic species in Q-space, and can be related to the radial distribution functions, $g_{\alpha\beta}(r)$, via a Fourier transformation:

$$S_{\alpha\beta}(Q) = 1 + 4\pi\rho \int_0^\infty r^2 [g_{\alpha\beta}(r) - 1] \frac{\sin(Qr)}{Qr} dr \qquad , \qquad \text{(Eq. 3)}$$

where ρ is the atomic density of the sample.

The key aim of most structural studies of liquids is to extract $g_{\alpha\beta}(r)$, the function representing real space correlations between atom pairs as a function of the separation, r, between them. The cumulative coordination number of species β from species α at a distance r is given as $N_{\alpha\beta}(r)$ and can be found using:

$$N_{\alpha\beta}(r) = \int_0^r g_{\alpha\beta}(r) \, \rho_\beta \cdot 4\pi r^2 dr. \qquad \qquad (7)$$

To enable the full extraction of interatomic structural correlations, or partial pair distribution functions, a series of diffraction experiments is required. Measurement of several

isotopomeric samples varies the contrast of the total structure factor, allowing for multiple diffraction patterns of a specific system to be measured. Hydrogen/deuterium isotopic substitution augmented with neutron diffraction is a powerful probe of local structure, since the largely contrasting neutron scattering lengths delineates the various site-site distributions necessary to describe the local interactions in a liquid.

SI II: Experimental Methods

Neutron diffraction experiments were performed using the NIMROD instrument at the ISIS spallation neutron source (RAL, STFC, UK)[1]. This diffractometer was purposefully built and optimized for structural study of hydrogen-containing disordered materials. To enable the extraction of intermolecular structure correlations between NMP molecules, data were measured for three samples:

(1) protiated NMP, C_4H_9NO;

(2) deuterated NMP, C_4D_9NO; and

(3) a 1:1 mixture of C_4H_9NO and C_4D_9NO,

over the Q range 0.02 Å < Q < 50Å. The complementarity of the extracted data sets are constraints for structure refinement methods (see 'EPSR Modelling' section).

Samples were prepared and contained in flat-plate null scattering $Ti_{0.68}Zr_{0.32}$ alloy cells of internal dimensions 1 mm x 35 mm x 35 mm. This null-scattering alloy composition ensures that the cell does not contribute any coherent neutron scattering to the measured signal. Scattering from the empty sample cells, as well as the empty instrument, were collected for data corrections. Data was then normalized, calibrated and put on an absolute scale by comparison with the scattering from 3mm vanadium-niobium plate. Particular attention was paid to correction of inelasticity effects, especially for the samples containing hydrogen. The self-scattering background and inelasticity effects were removed from the total differential scattering cross section using an iterative method developed by Soper[2,3].

SI III: EPSR Modelling

Empirical Potential Structure Refinement (EPSR) was used to build a three-dimensional model of liquid NMP that is consistent with the structure factors measured for the three samples: C_4H_9NO, C_4D_9NO and the 1:1 mixture of C_4H_9NO and C_4D_9NO. In the first instance, a combination of Lennard-Jones (LJ) and Coulomb potentials were used to build the following reference potential, $U_{\alpha\beta}(r)$, between atom pairs, α and β, in the molecule, represented by:

$$U_{\alpha\beta}(r) = 4\varepsilon_{\alpha\beta}\left[\left(\frac{\sigma_{\alpha\beta}}{r}\right)^{12} - \left(\frac{\sigma_{\alpha\beta}}{r}\right)^6\right] + \frac{1}{4\pi\varepsilon_0}\frac{q_\alpha q_\beta}{r} \qquad , \qquad \text{(Eq. 4)}$$

where $\varepsilon_{\alpha\beta}$ and $\sigma_{\alpha\beta}$ are computed using the classical Lorentz-Berthelot mixing rules for the cross terms, and ε_0 is the permittivity of free space.

The EPSR process begins with a standard Monte Carlo simulation, with traditional implementation of periodic boundary condition and the minimum image convention. A smooth truncation is applied to the Lennard-Jones potential energy functions, as detailed by Soper[4], using a function of the form:

$$T(r) = \begin{cases} 1 & r \leq r_1 \\ 0.5\left[1 + \cos\pi\left(\frac{r-r_1}{r_2-r_1}\right)\right] & r_1 < r < r_2 \\ 0 & r \geq r_2 \end{cases} \qquad , \qquad \text{(Eq. 5)}$$

where r_1 = 9Å and r_2 =12 Å. The Coulomb potentials are also truncated using the switching function:

$$T_c(r) = \left(1 - \frac{r}{r_2}\right)^4\left(1 + \frac{8r}{5r_2} + \frac{2r^2}{5r_2{}^2}\right)\theta(r_2 - r) \qquad , \qquad \text{(Eq. 6)}$$

derived by Hummer *et al.* within the reaction field approximation, with $\theta(r_2 - r)$ being the Heaviside step function.[5]

Table S1. Reference Seed Potentials for all of the labelled atoms in the EPSR model of liquid NMP, showing Lennard-Jones well-depth parameter, atomic mass and charge.

Atom type	$\varepsilon\,/\,kJ\,mol^{-1}$	$\sigma\,/\,\text{Å}$	q_e
C1	0.43932	3.7500	0.2614
H_{ring}	0.12552	2.5000	0.0589
C2	0.27614	3.5000	- 0.1179
C3	0.27614	3.5000	- 0.0696
N1	0.71128	3.2500	- 0.0769
O1	0.87864	2.9600	- 0.3480
C4	0.27614	3.5000	- 0.0613
H_{Me}	0.12552	2.5000	0.0589

For the simulation, a cubic box of side length 54.29 Å containing 1000 NMP molecules with an atomic density of 0.10008 Å^{-1} at 298 K was used, seeded by pairwise (Lennard-Jones and Coulomb) potentials. Atom-centred OPLS force-field parameters were used -- these are summarized in Table S1. The labels assigned to atomic sites on the NMP molecule are shown in Figure S2. Using the seed potentials, standard Metropolis Monte Carlo steps are used to bring the simulation to equilibrium. Once equilibrated, structure refinement is initialized. During this process, the interatomic site-site potentials are iteratively refined to drive the simulated structure toward agreement with the experimental data. This achieved through modification of an additional empirical potential, based on the difference between measured and simulated structure factors. This allows molecular and electronic information known *a priori* to be built into the refinement procedure. Once a reasonable agreement is achieved, the simulation is allowed to proceed without further perturbation of the potentials. Ensemble average structural information is then accumulated.
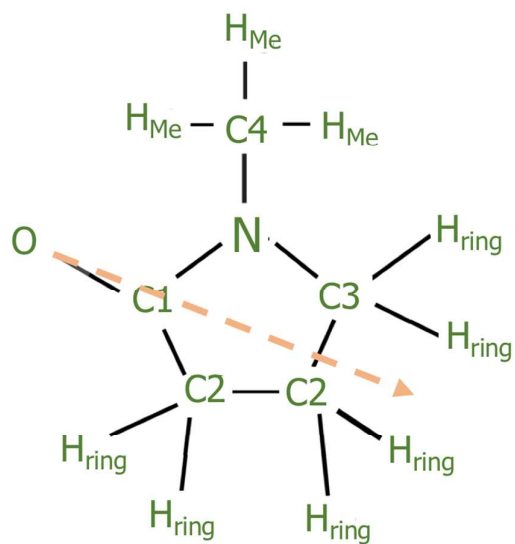
Figure S2. Atom numbering scheme for the NMP molecule in the present work. The arrow indicates the dipole moment in the molecule[6].

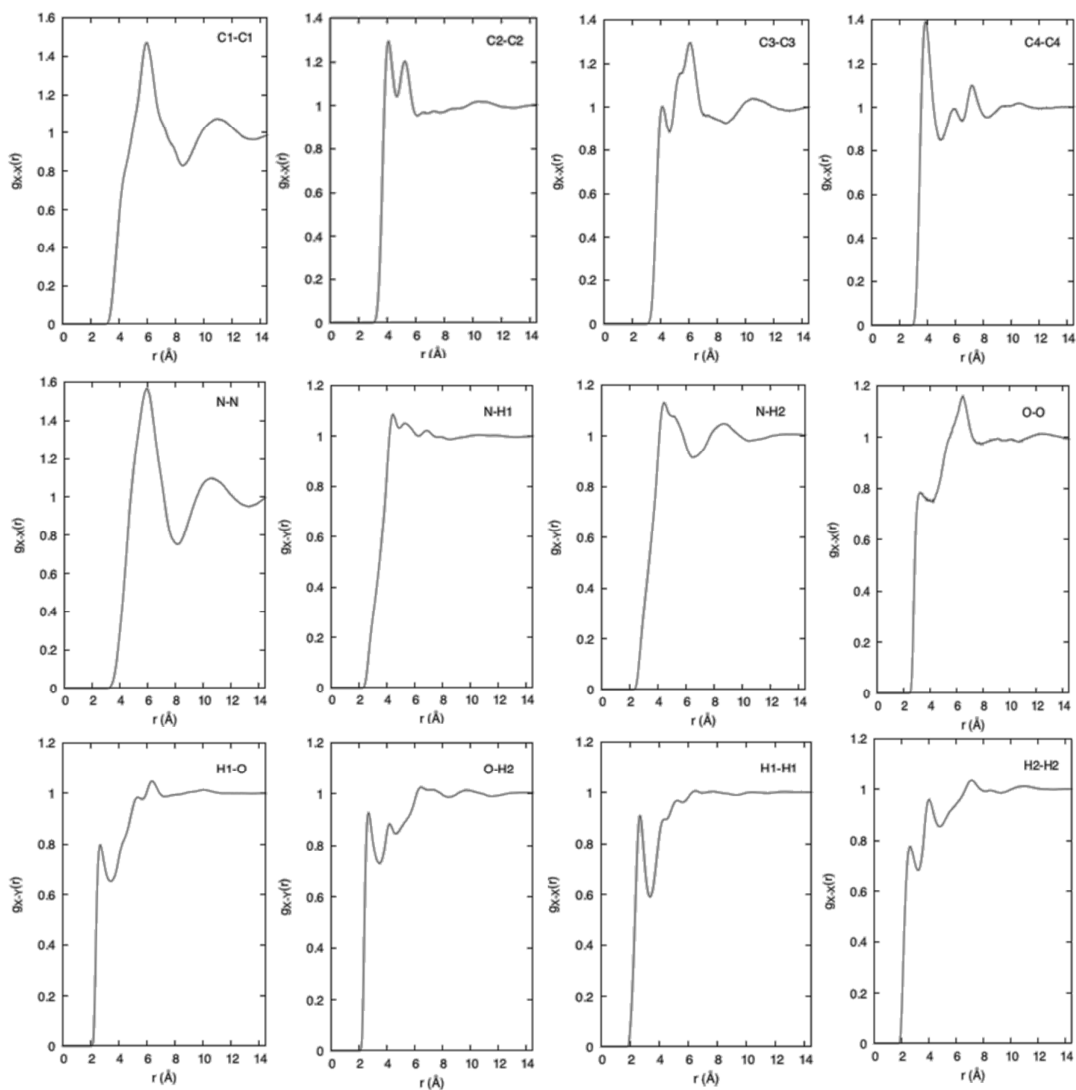**SI IV: Selected site-site intermolecular partial distribution functions for NMP**

Figure S3: EPSR-derived site-site intermolecular partial distribution functions for NMP at room temperature: C1-C1, C2-C2, C3-C3, C4-C4, N-N, N-H1, N-H2, O-O, H1-O, O-H2, H1-H1 and H2-H2. Here, H_1 and H_2 and the H_{ring} and H_{Me} atoms, respectively.

SI V: Coordination Numbers

Coordination numbers for the first shell were calculated by integration of the area underneath the RDF's first peak and are also given in Table S2.

Table S2: Relevant Coordination Numbers Obtained by Integration of the Features in the Indicated Partial Distribution Functions

Correlation	r_{min} (Å)	r_{max} (Å)	CN (atoms)
C1-H$_{ring}$	2.47	6.35	2.9
C1-H$_{Me}$	2.47	6.26	2.9
C2-H$_{Me}$	2.47	3.95	0.9
	3.95	5.42	1.4
N-N	3.31	8.05	4.5
N-O	2.72	4.97	1.5
	4.97	6.05	1.1
N-H$_{ring}$	2.39	4.89	1.5
N-H$_{Me}$	2.37	6.39	3.1
O-O	2.49	4.17	1.04
O-H$_{ring}$	2.11	3.46	0.78
O-H$_{Me}$	2.11	3.50	0.93

SI VI: Spatial Density Functions

Since site-site RDF's only give a one-dimensional representation of the liquid, using them to visualize spatial and orientational structure in three dimensions is difficult. Therefore, spatial density functions (SDFs) are constructed to represent a three-dimensional map of the density of neighboring molecule centers around an oriented central molecule, as a function of angular distance, r, and angular position. As opposed to 1-dimensional histogram binning in the case of the radial distribution function, SDFs are calculated from spatial probability densities of molecules around other molecules and amounts to performing three-dimensional histogram binning. The SDF thus shows regions of space around a central molecule that are most likely to be occupied between a specified distance range. For all SDFs shown herein, the central molecule's orientation was fixed by defining two axes: an x-axis from atom C3 to C1, and a y-axis from N to C4. The z-axis is then formed from the cross product of the x and y axes, thus effectively fixing the specified atoms as a point of reference for the central molecule.

SI VII. Extent of hydrogen bonding in NMP: The directionality of the C-O----H intermolecular angle

The recent IUPAC recommendation[7] on the definition of hydrogen bonding points to directionality as a key defining characteristic. In a strong hydrogen bond, intermolecular angle X-H----Y is generally linear or 180°, with a recommended lower limit of 110° for this angle. In light of this, a histogram of the intermolecular bond angles between the four atoms constituting the potentially hydrogen bond donating and accepting groups was computed. The data was then converted to a probability function shown in Figure S4. As expected, angles below 90 degrees are highly sterically constrained due to the presence of the rest of the molecule. For angles ranging between 90 and 180 degrees, there is an almost constant probability and thus there is no indication of a preferred direction which would be expected for a strong hydrogen bond.
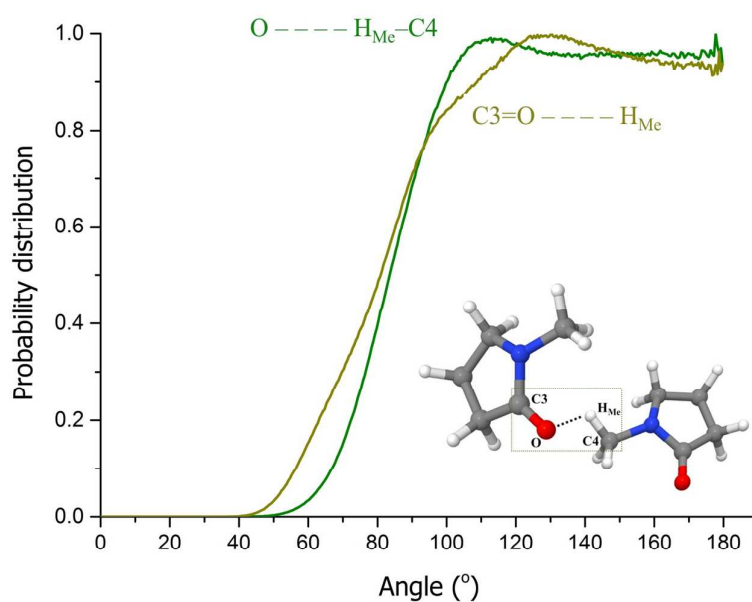

Figure S4: Probability density function showing the most probable angles for the intermolecular bond angle investigated herein. The pdf shows a wide range of conformation angles.

SI VIII. Orientational Correlation functions

Further detail about the relative arrangements of the nearest neighbor NMP can be extracted by examination of orientational correlation functions, e.g. the angular radial distribution functions (aRDF). The aRDF, $g(r,\theta)$, is the RDF plotted as a function of the angle between the z-axes of the central and surrounding molecules[8], and defined as:

$$g(r,\theta) = \frac{\Delta n(r,\theta)}{\frac{2}{3}\pi((r+\Delta r)^3 - r^3).\sin\theta.\Delta\theta.\rho} \qquad \text{(Eq. 4)}$$

where $\Delta n(r,\theta)$ is the number of molecules in distance range r+Δr and angle range $\theta + \Delta\theta$, ρ is the molecular number density, the $1/(\sin\theta)$ factor corrects for the θ-dependence of the solid angle as we integrate over the azimuthal angle.

An exemplar coordinate axes reference frame which was used in the NMP ring-centre–ring-centre angular radial distribution analysis is given in Figure S6.
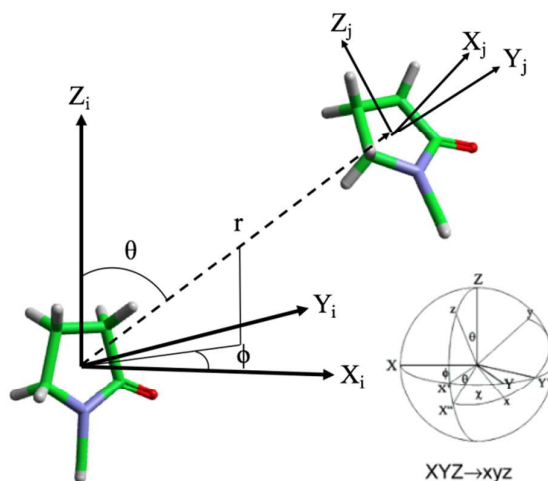

Figure S6. Coordinate axes reference frames of two NMP molecules, i and j, used in the NMP ring centre–ring centre orientational correlation analysis, showing relative molecular orientations and defining the angle theta. The inset coordinate axes (from Ref (9)) illustrates the transformation scheme characterized by the Euler angle convention used to go from the frame of reference XYZ to xyz.

References

(1)   Bowron, D. T.; Soper, A. K.; Jones, K.; Ansell, S.; Birch, S.; Norris, J.; Perrott, L.; Riedel, D.; Rhodes, N. J.; Wakefield, S. R.; et al. NIMROD: The Near and InterMediate Range Order Diffractometer of the ISIS Second Target Station. *Rev. Sci. Instrum.* **2010**, *81*, 33905.

(2)   Soper, a. K. Inelasticity Corrections for Time-of-Flight and Fixed Wavelength Neutron Diffraction Experiments. *Mol. Phys.* **2009**, *107*, 1667–1684.

(3)   Soper, A. K.; K., A. The Radial Distribution Functions of Water as Derived from Radiation Total Scattering Experiments: Is There Anything We Can Say for Sure? *ISRN Phys. Chem.* **2013**, *2013*, 1–67.

(4)   Soper, a. K. Tests of the Empirical Potential Structure Refinement Method and a New Method of Application to Neutron Diffraction Data on Water. *Mol. Phys.* **2001**, *99*, 1503–1516.

(5)   Hummer, G.; Pratt, L. R.; Garcia, A. E. Hydration Free Energy of Water. *J. Phys. Chem.*, **1995**, *99*, 14188–14194.

(6)   Aparicio, S.; Alcalde, R.; Dávila, M. J.; García, B.; Leal, J. M. Measurements and Predictive Models for the N -Methyl-2-pyrrolidone/Water/Methanol System. *J. Phys. Chem. B* **2008**, *112*, 11361–11373.

(7)   Arunan, E.; Desiraju, G. R.; Klein, R. A.; Sadlej, J.; Scheiner, S.; Alkorta, I.; Clary, D. C.; Crabtree, R. H.; Dannenberg, J. J.; Hobza, P.; et al. Defining the Hydrogen Bond: An Account (IUPAC Technical Report). *Pure Appl. Chem.* **2011**, *83*, 1619–1636.

(8)   Youngs, T. G. A. Aten - An Application for the Creation, Editing, and Visualization of Coordinates for Glasses, Liquids, Crystals, and Molecules. *J. Comput. Chem.* **2010**, *31*, 639–648.

(9)   Bowron, D. T.; Finney, J. L.; Soper, A. K. The Structure of Liquid Tetrahydrofuran. *J. Am. Chem. Soc.* **2006**, *128*, 5119–5126.